Rencontres de Moriond - EW Interactions and Unified Theories
La Thuile, March 15-22, 2014

Latest results on radiative penguin decays at BABAR

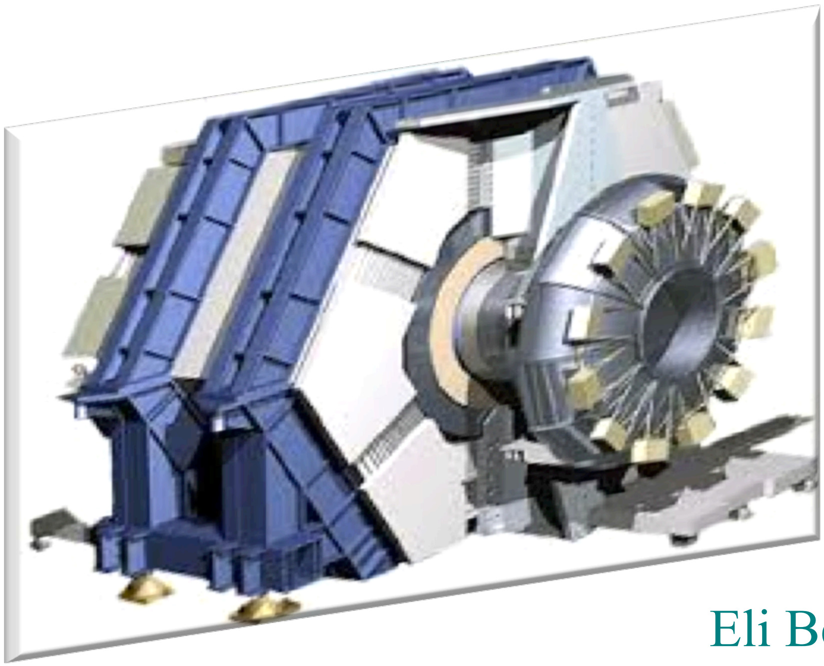

Eli Ben-Haïm
LPNHE-IN2P3-
Université Pierre et Marie Curie (Paris)
On behalf of the ***BABAR*** collaboration

LPNHE PARIS

BABAR

Introduction and overview

Study of the $K\pi\pi$ resonant system (Branching fractions)

$B^+ \rightarrow K^+\pi^-\pi^+\gamma$

input

$B^0 \rightarrow K_S\pi^+\pi^-\gamma$

Mixing induced CP violation (S)

première!

$B \rightarrow X_s\, \ell^+\ell^-$

Branching fractions

Direct CP asymmetry

première!

Confront standard model (SM) predictions

Constrain the parameter space of new physics (NP) models

All the results presented here are preliminary (not yet published)

- Modes with branching fractions (BF) of ~ 10^{-5} to 10^{-6} in the standard model (SM)
- New physics (NP) could significantly alter BF and CP asymmetries
- Challenge: small theoretical & experimental uncertainties for powerful comparison

b→ s γ(ℓℓ): FCNC processes

- Within the SM, these processes proceed via loop/box diagrams like

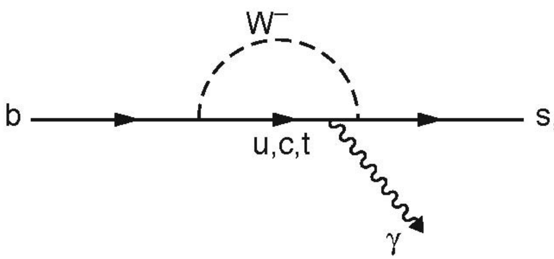

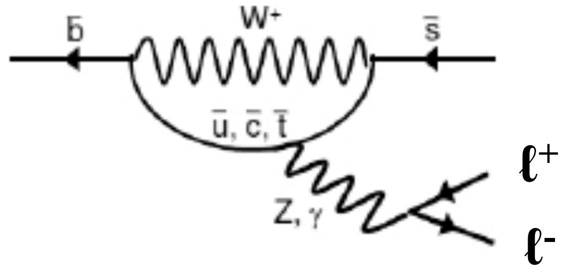

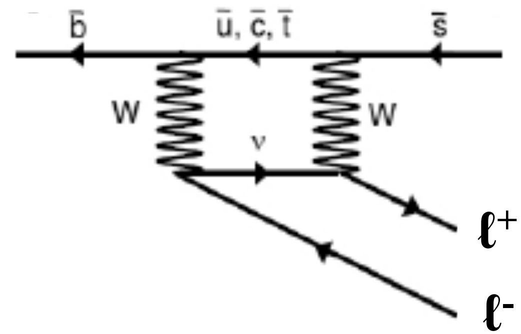

- Examples for NP scenarios

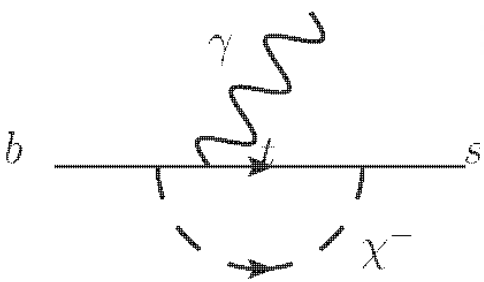

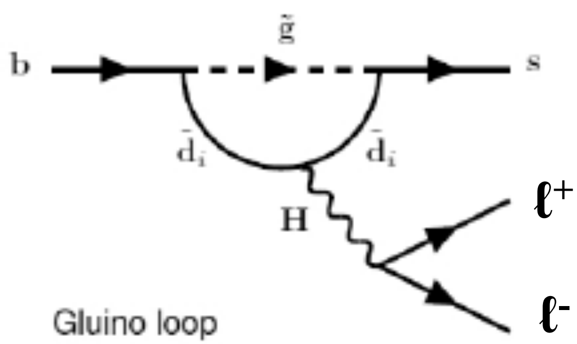

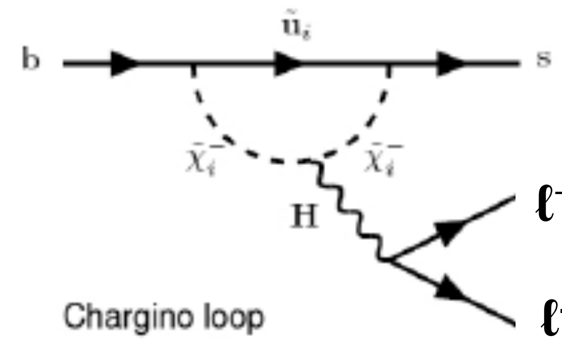

+ ?

The BaBar detector and dataset

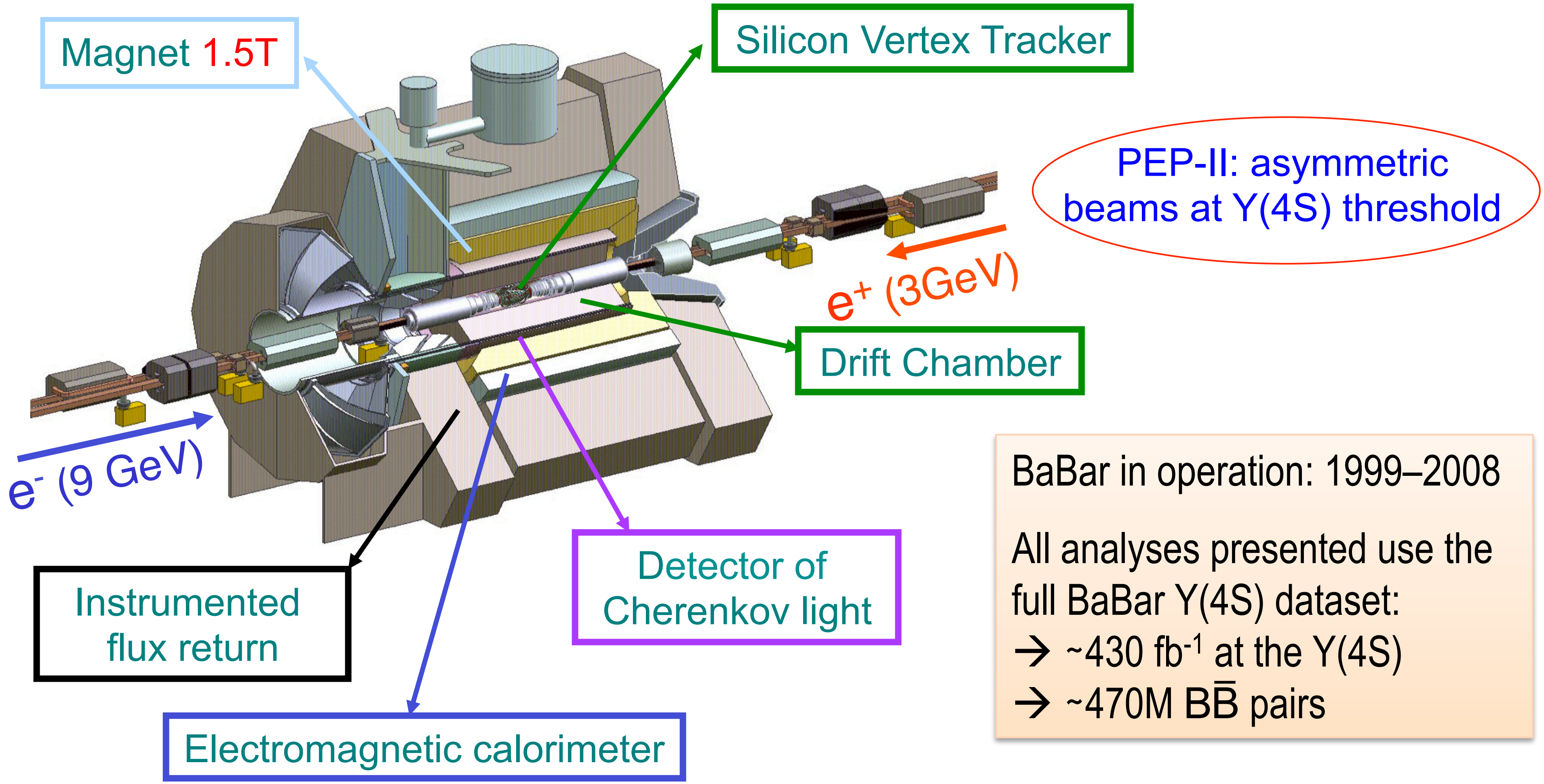

BaBar in operation: 1999–2008

All analyses presented use the full BaBar Y(4S) dataset:
→ ~430 fb^{-1} at the Y(4S)
→ ~470M $B\bar{B}$ pairs

BaBar is well suited for the measurements of our modes of interest: hermetic detector, clean environment, good K_S and π^0 reconstruction

Common analysis techniques

Kinematics of fully reconstructed B

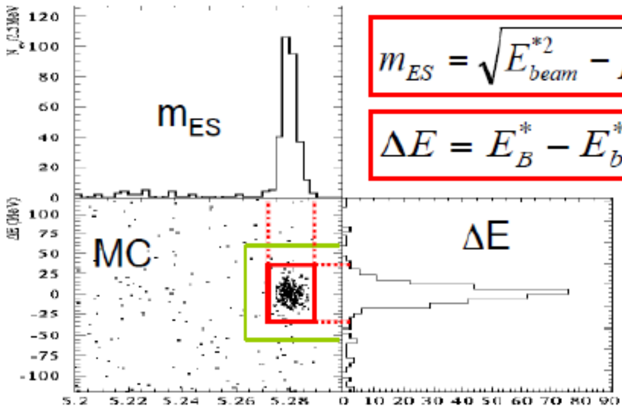

$$m_{ES} = \sqrt{E_{beam}^{*2} - p_B^{*2}}$$

$$\Delta E = E_B^* - E_{beam}^*$$

Good charged particle ID (in particular K/π) up to few GeV/c

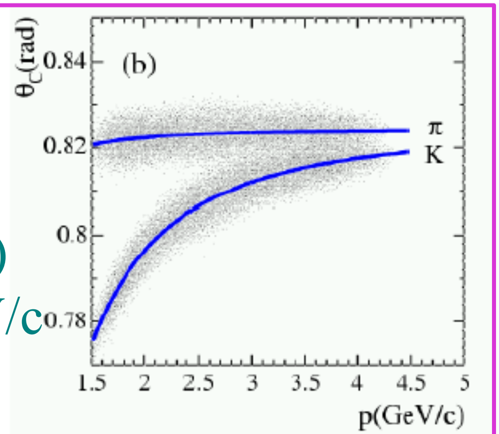

Background characterization:

→ Mainly continuum: $e^+e^- \to q\bar{q}$ (q = u,d,s,c).

Suppression by multi-variable classifiers based on event-shape variables:

Fisher discriminant, Boosted decision trees (BDT) …

Topology:

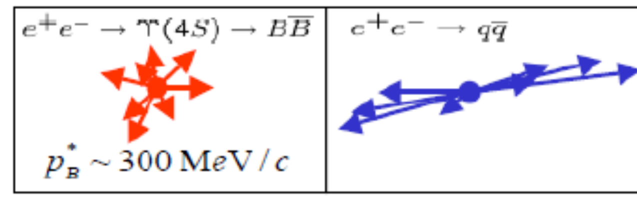

Angular distribution:

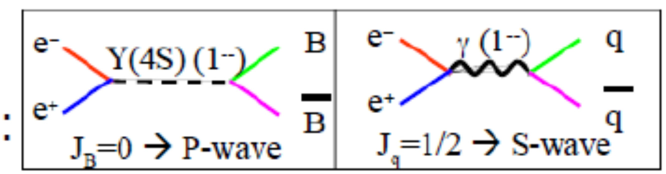

→ Background from B decays: classified by kinematic and topological properties

Variables are often combined to a likelihood function, used in a maximum likelihood fit for signal/background separation and to measure parameters of interest

$B \to X_s \ell^+ \ell^-$

Measurement of branching fractions and search for direct CP violation from a sum of exclusive final states

arXiv:1312.5364 [hep-ex], To be submitted to Phys.Rev.Lett

Analysis method (I)

- The $\ell^+\ell^-$ pair is $\mu^+\mu^-$ or e^+e^-
- X_s = sum of **10** exclusive states (m(Xs) < 1.8 GeV):
  - 0 pions: K_S ($\to \pi^+\pi^-$), K^+
  - 1 pion: $K_S\pi^0$, $K_S\pi^+$, $K^+\pi^0$, $K^+\pi^+$
  - 2 pions: $K_S\pi^0\pi^+$, $K_S\pi^+\pi^-$, $K^+\pi^0\pi^+$, $K^+\pi^+\pi^-$

    → rates of related modes ($K_S \to \pi^0\pi^0$, K_L…) inferred

Optimization studied

Represents ~70% of the inclusive rate in $m(X_s)$ < 1.8 GeV

Extrapolation of missing modes and mass range: simulated events (JETSET)

- $X_s e^+e^-$ and $X_s\mu^+\mu^-$ rates extracted independently in hadronic mass (M_x) and $m^2(\ell^+\ell^-) \equiv q^2 = s$ bins

  ⇒ $BF(q^2)$, $BF(M_x)$
- Separate B and $\bar{B}$ rates in $m^2(\ell^+\ell^-)$ bins for the **7** self-tagging modes above

  ⇒ $A_{CP}(q^2)$
- J/ψ and $\psi(2S) \to \ell^+\ell^-$ are vetoed and used as control samples

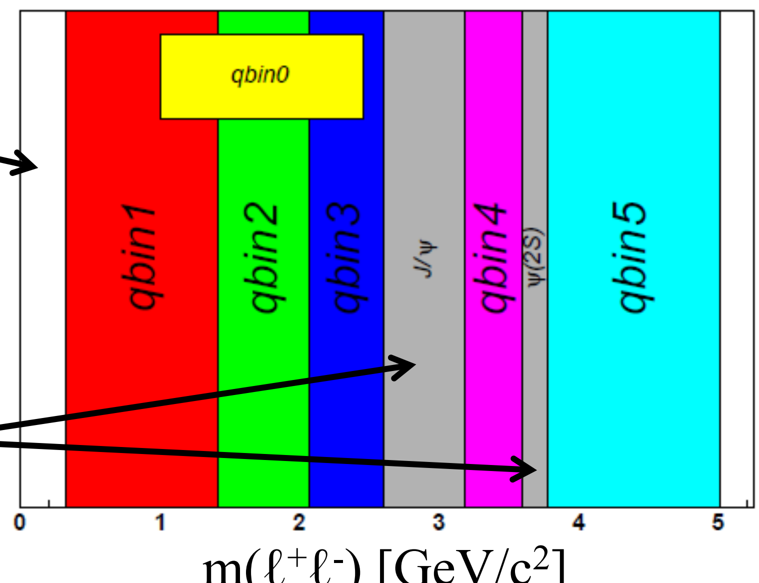

Analysis method (I)

- The $\ell^+\ell^-$ pair is $\mu^+\mu^-$ or e^+e^-
- X_s = sum of **10** exclusive states (m(Xs) < 1.8 GeV):
  - 0 pions: K_S ($\to \pi^+\pi^-$), K^+
  - 1 pion: $K_S\pi^0$, $K_S\pi^+$, $K^+\pi^0$, $K^+\pi^+$
  - 2 pions: $K_S\pi^0\pi^+$, $K_S\pi^+\pi^-$, $K^+\pi^0\pi^+$, $K^+\pi^+\pi^-$

  → rates of related modes ($K_S \to \pi^0\pi^0$, K_L…) inferred

Optimization studied

Represents ~70% of the inclusive rate in $m(X_s) < 1.8$ GeV

Extrapolation of missing modes and mass range: simulated events (JETSET)

- $X_s e^+e^-$ and $X_s\mu^+\mu^-$ rates extracted independently in hadronic mass (M_x) and $m^2(\ell^+\ell^-) \equiv q^2 = s$ bins

  ⇒ **BF(q^2), BF(M_x)**
- Separate B and $\bar{B}$ rates in $m^2(\ell^+\ell^-)$ bins for the **7** self-tagging modes above

  ⇒ **$A_{CP}(q^2)$**
- J/ψ and $\psi(2S) \to \ell^+\ell^-$ are vetoed and used as control samples

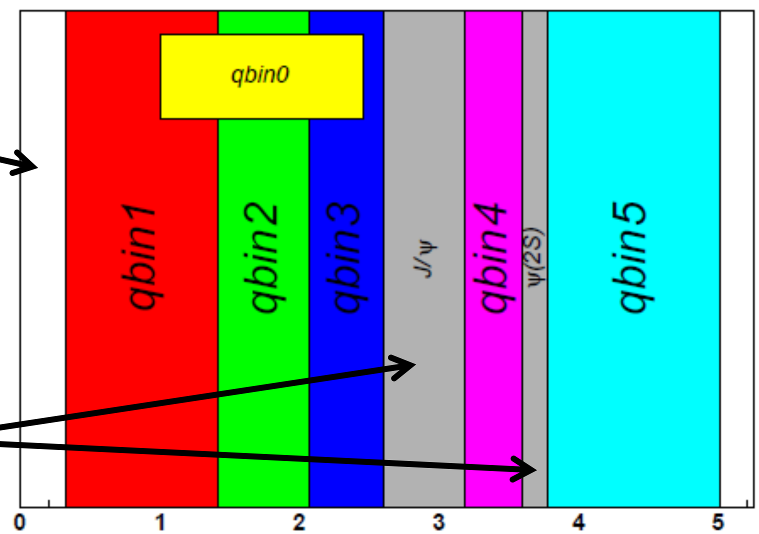

Analysis method (II)

- Extraction of signal yields in the different bins by 2D maximum likelihood fit to m_{ES} and a likelihood ratio (LHR) built from boosted decision trees

Example of signal enhanced fit projection (all $\mu^+\mu^-$ modes) for the first q bin

0.316 < q <1.414 GeV/c

Signal m_{ES} peaks at m_B

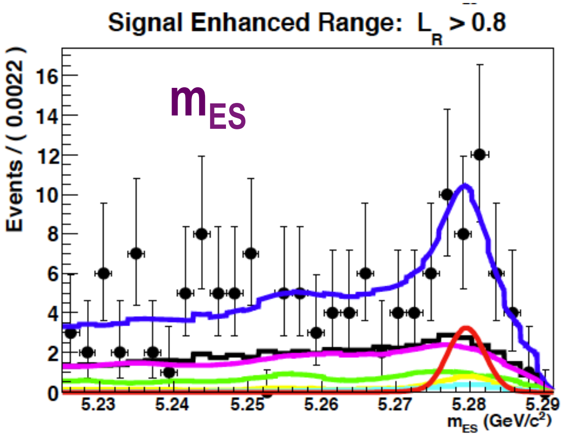

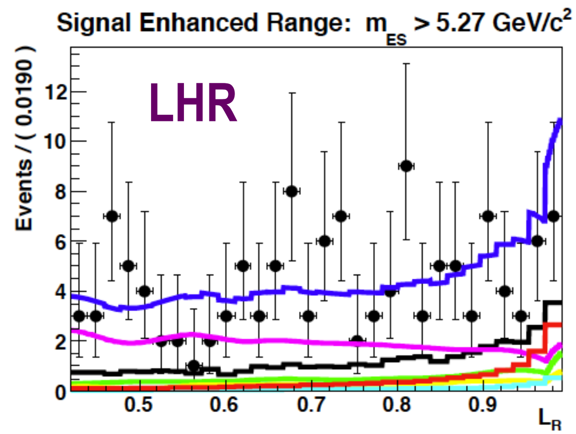

Signal LHR peaks at 1

Preliminary

BF extracted from likelihood profile

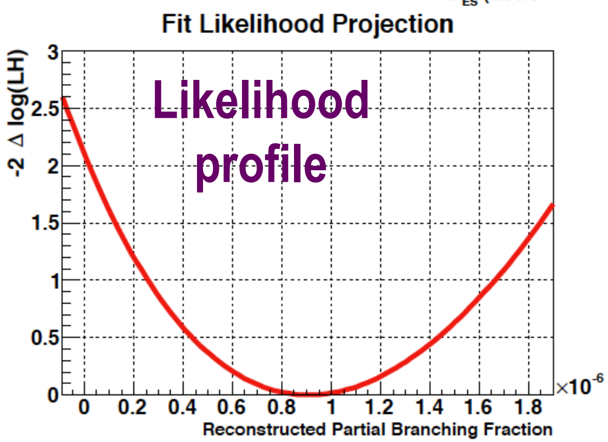

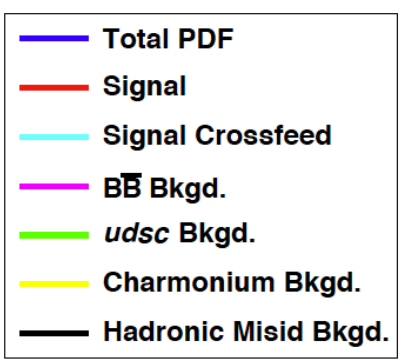

4 background categories

Results (I)

Total and partial BF (x 10^{-6}) (Preliminary)

Bin	Range	$B \to X_s e^+ e^-$	$B \to X_s \mu^+ \mu^-$	$B \to X_s \ell^+ \ell^-$
q_0^2	$1.0 < q^2 < 6.0$	$1.93^{+0.47+0.21}_{-0.45-0.16} \pm 0.18$ (1.71)	$0.66^{+0.82+0.30}_{-0.76-0.24} \pm 0.07$ (1.78)	$1.60^{+0.41+0.17}_{-0.39-0.13} \pm 0.18$
q_1^2	$0.1 < q^2 < 2.0$	$3.05^{+0.52+0.29}_{-0.49-0.21} \pm 0.35$ (1.96)	$1.83^{+0.90+0.30}_{-0.80-0.24} \pm 0.20$ (2.02)	$2.70^{+0.45+0.21}_{-0.42-0.16} \pm 0.35$
q_2^2	$2.0 < q^2 < 4.3$	$0.69^{+0.31+0.11}_{-0.28-0.07} \pm 0.07$ (1.73)	$-0.15^{+0.50+0.26}_{-0.43-0.14} \pm 0.01$ (1.80)	$0.46^{+0.26+0.10}_{-0.23-0.06} \pm 0.07$
q_3^2	$4.3 < q^2 < 6.8$	$0.69^{+0.31+0.13}_{-0.29-0.10} \pm 0.05$ (1.53)	$0.34^{+0.54+0.19}_{-0.50-0.15} \pm 0.03$ (1.59)	$0.60^{+0.27+0.10}_{-0.25-0.08} \pm 0.05$
q_4^2	$10.1 < q^2 < 12.9$	$1.14^{+0.42+0.22}_{-0.40-0.10} \pm 0.04$ (1.16)	$0.87^{+0.51+0.11}_{-0.47-0.08} \pm 0.03$ (1.18)	$1.02^{+0.32+0.10}_{-0.30-0.07} \pm 0.04$
q_5^2	$14.2 < q^2$	$0.56^{+0.19+0.03}_{-0.18-0.03} \pm 0.00$ (1.02)	$0.60^{+0.31+0.05}_{-0.29-0.04} \pm 0.00$ (1.02)	$0.57^{+0.16+0.03}_{-0.15-0.02} \pm 0.00$
$m_{X_s,1}$	$0.4 < m_{X_s} < 0.6$	$0.69^{+0.18+0.04}_{-0.17-0.03} \pm 0.00$ (1.00)	$0.74^{+0.25+0.04}_{-0.23-0.04} \pm 0.00$ (1.00)	$0.71^{+0.15+0.03}_{-0.14-0.03} \pm 0.00$
$m_{X_s,2}$	$0.6 < m_{X_s} < 1.0$	$1.20^{+0.34+0.10}_{-0.33-0.07} \pm 0.00$ (1.00)	$0.76^{+0.44+0.08}_{-0.40-0.07} \pm 0.00$ (1.00)	$1.02^{+0.27+0.06}_{-0.25-0.05} \pm 0.00$
$m_{X_s,3}$	$1.0 < m_{X_s} < 1.4$	$1.60^{+0.72+0.27}_{-0.69-0.19} \pm 0.05$ (1.18)	$0.65^{+1.16+0.27}_{-1.08-0.25} \pm 0.02$ (1.18)	$1.32^{+0.61+0.19}_{-0.58-0.15} \pm 0.05$
$m_{X_s,4}$	$1.4 < m_{X_s} < 1.8$	$1.88^{+0.76+0.71}_{-0.73-0.47} \pm 0.12$ (1.91)	$0.19^{+1.35+0.70}_{-1.25-0.50} \pm 0.10$ (1.91)	$1.36^{+0.67+0.50}_{-0.63-0.34} \pm 0.12$
Total	$0.1 < q^2$	$7.69^{+0.82+0.50}_{-0.77-0.33} \pm 0.50$	$4.41^{+1.31+0.57}_{-1.17-0.42} \pm 0.27$	$6.73^{+0.70+0.34}_{-0.64-0.25} \pm 0.50$

Stat.

Experimental syst.

Model syst.

Extrapolation factor to account for unmeasured modes

A few results are commented in the next slide

Relative precision improved by a factor ~2 wrt previously published measurements

(Estimated contributions from vetoed charmonium mass regions included in total results)

Results (II)

$B \to X_s \ell^+ \ell^-$

Branching fractions

- In $q^2 > 0.1$ GeV^2/c^4 (same units elsewhere)

$$\mathcal{B}(B \to X_s \ell^+ \ell^-) = (6.73^{+0.70+0.34}_{-0.63-0.25} \pm 0.5) \times 10^{-6}$$

$$\mathcal{B}_{SM}(B \to X_s \ell^+ \ell^-) = (4.6 \pm 0.8) \times 10^{-6} \quad (1)$$

→ < 2σ higher than the SM prediction

- In the low mass region $1 < q^2 < 6$

$$\mathcal{B}(B \to X_s \ell^+ \ell^-) = (1.60^{+0.41+0.17}_{-0.39-0.13} \pm 0.18) \times 10^{-6}$$

$$\mathcal{B}_{SM}(B \to X_s e^+ e^-) = (1.64 \pm 0.11) \times 10^{-6} \quad (2)$$

→ in good agreement with the SM

- In the high mass region $q^2 > 14.2$

$$\mathcal{B}(B \to X_s \ell^+ \ell^-) = (0.57^{+0.16+0.03}_{-0.15-0.02} \pm 0.0) \times 10^{-6}$$

$$\mathcal{B}_{SM}(B \to X_s e^+ e^-) = (0.21 \pm 0.07) \times 10^{-6} \quad (2)$$

→ ~2σ higher than SM prediction

→ > 2σ away from the prediction related to the δC_9 NP interpretation of the recently reported LHCb P_5' anomaly in $B^0 \to K^* \mu^+ \mu^-$

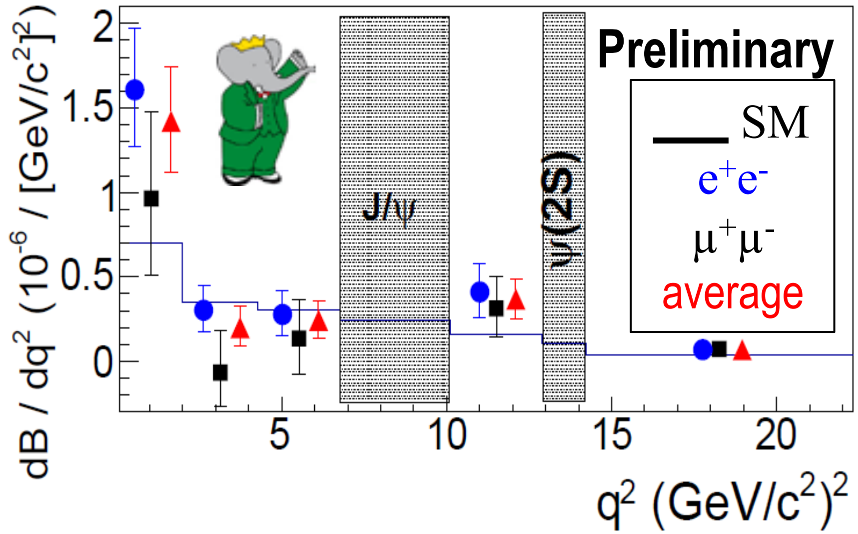

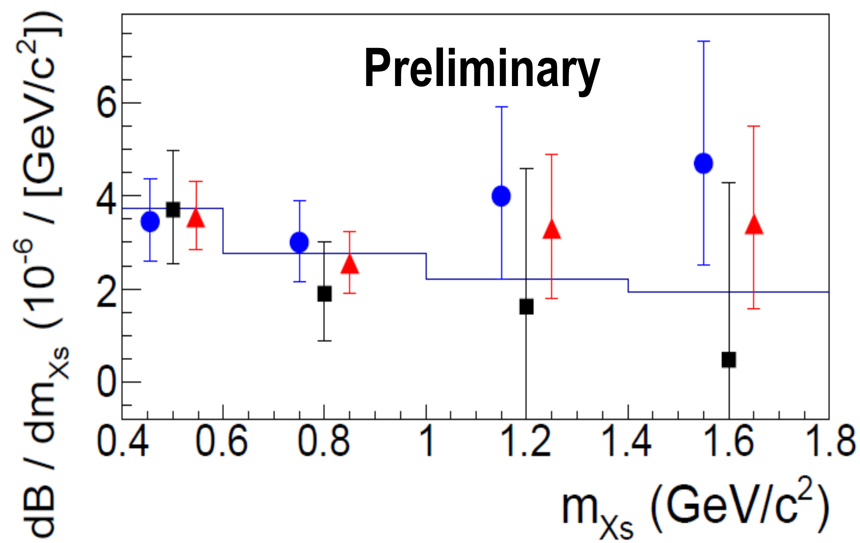

(1) Nucl.Phys.B 685, 351 (2004) (2) Nucl.Phys.B 802, 40 (2008)

Results (III)

CP Asymmetry

Integrated A_{CP}:

$0.04 \pm 0.11 \pm 0.01$

in agreement with SM prediction:

$0.0019^{+0.0017}_{-0.0019}$

(1) Phys. Rev. D 54, 882 (1996)
(2) Eur. Phys. J C 8, 619 (1999)

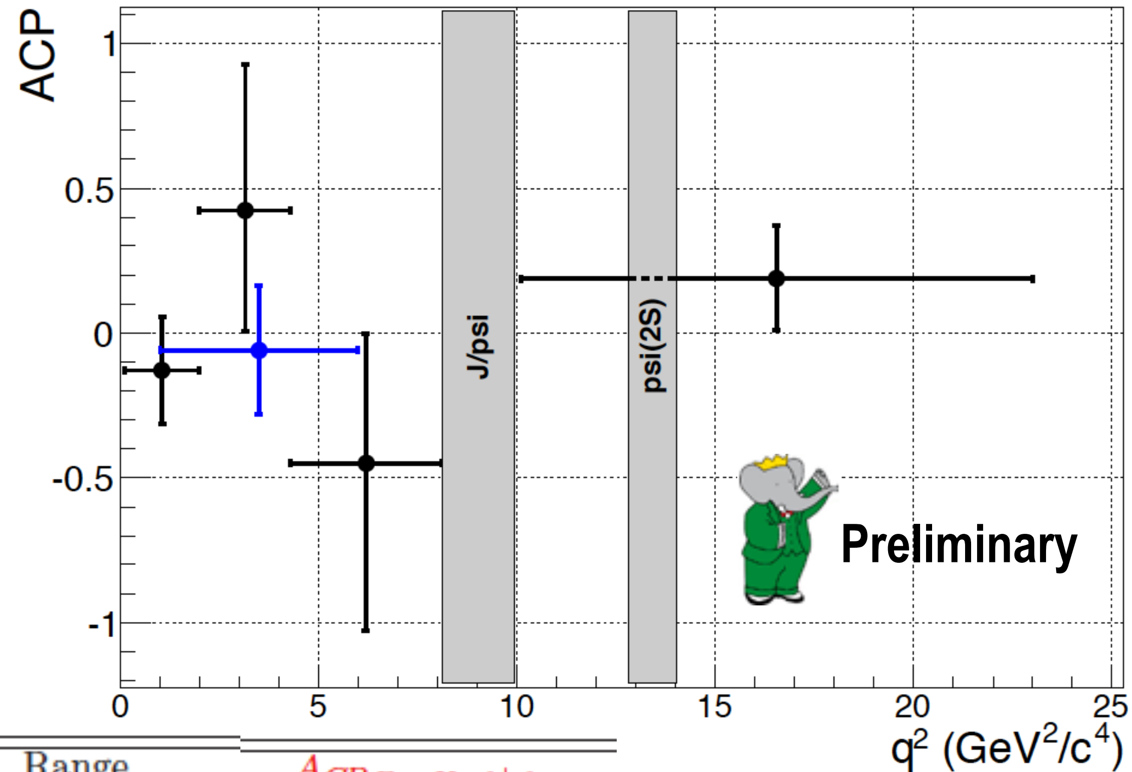

Bin	Range	$A_{CP\,B \to X_s \ell^+ \ell^-}$
q_0^2	$1.0 < q^2 < 6.0$	$-0.06 \pm 0.22 \pm 0.01$
q_1^2	$0.1 < q^2 < 2.0$	$-0.13 \pm 0.18 \pm 0.01$
q_2^2	$2.0 < q^2 < 4.3$	$0.42^{+0.50}_{-0.42} \pm 0.01$
q_3^2	$4.3 < q^2 < 6.8$	$-0.45^{+0.44}_{-0.57} \pm 0.01$
q_4^2	$10.1 < q^2 < 12.9$	
q_5^2	$14.2 < q^2$	
q_{45}^2	$q_4^2 + q_5^2$	$0.19^{+0.18}_{-0.17} \pm 0.01$

merged

$B \to K\pi^+\pi^-\gamma$

- Time dependent analysis of $B^0 \to K_S\pi^+\pi^-\gamma$ and studies of the $K^+\pi^-\pi^+$ system in $B^+ \to K^+\pi^-\pi^+\gamma$ decays

Paper in preparation, to be submitted to Phys.Rev.D

Fundamentals

- SM: left-handed quarks and right-handed antiquarks

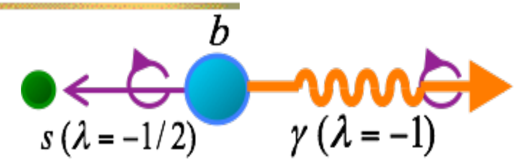

- NP particle may be present in the loop and enhance right-handed photons

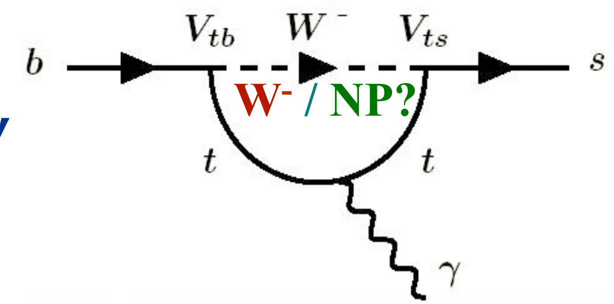

SM $\Rightarrow$ $b \to s\gamma_L$ or $\bar{b} \to \bar{s}\gamma_R$ $\Rightarrow$

CP asymmetry parameters ≈ 0

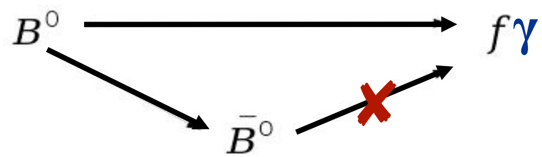

NP $\Rightarrow$ $b \to s\gamma_{L,R}$ or $\bar{b} \to \bar{s}\gamma_{R,L}$ $\Rightarrow$

CP asymmetry parameters ≠ 0

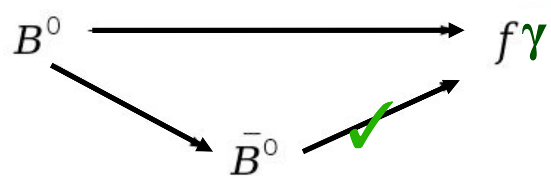

$$\begin{aligned}\mathcal{A}_{CP}(\Delta t) &= \frac{\Gamma(\overline{B}^0(\Delta t) \to f_{CP}\gamma) - \Gamma(B^0(\Delta t) \to f_{CP}\gamma)}{\Gamma(\overline{B}^0(\Delta t) \to f_{CP}\gamma) + \Gamma(B^0(\Delta t) \to f_{CP}\gamma)} \\ &= \mathcal{S}_{f_{CP}} \sin(\Delta m_d \Delta t) - \mathcal{C}_{f_{CP}} \cos(\Delta m_d \Delta t)\end{aligned}$$

Observable

$$\mathcal{S}_{f_{CP}} \overset{\text{SM}}{\propto} \frac{m_s}{m_b} \simeq 0.02$$

Objective: measurement of $\mathcal{S}$ in $B^0 \to K_S \rho \gamma$ decays

Strategy (I)

- Difficulty: irreducible contribution from non CP eigenstates

$B^0 \to K_S\, \rho^0(\to \pi^-\pi^+)\, \gamma$:

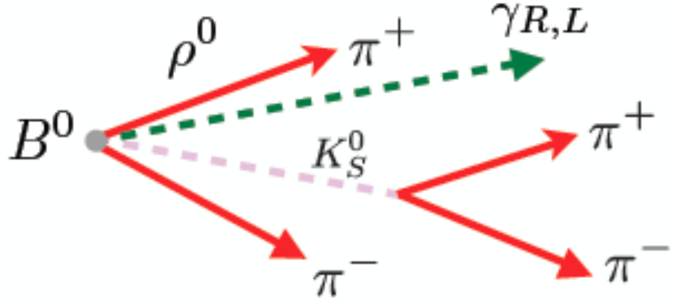

$B^0 \to K^{*\pm}(\to K_S\, \pi^\pm)\, \pi^\mp\, \gamma$:

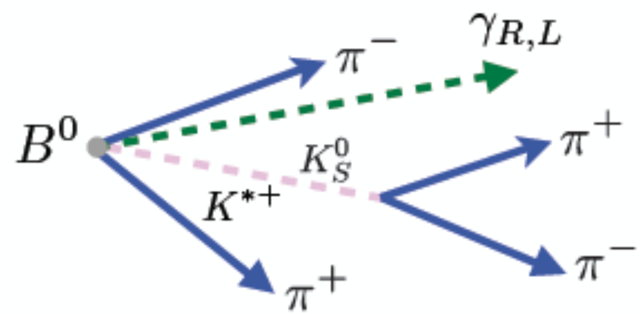

$\Rightarrow$ An amplitude analysis is necessary to extract a dilution factor:

$$\boxed{\mathcal{D}_{K_S^0\rho\gamma}} \equiv \frac{\boxed{\mathcal{S}_{K_S^0\pi^+\pi^-\gamma}}}{\boxed{\mathcal{S}_{K_S^0\rho\gamma}}}$$

- As there are not enough $B^0 \to K_S\pi^+\pi^-\gamma$ signal events to perform this amplitude analysis, D is extracted from $B^+ \to K^+\pi^-\pi^+\gamma$ decays, assuming isospin asymmetry.
- Further difficulty: due to the 4-body final state the kinematic boundaries of the ($K\pi$ - $\pi\pi$) phase space vary event by event.

Strategy (II)

Three stages of the $\mathbf{B^+ \to K^+\pi^-\pi^+\gamma}$ analysis

(1) Maximum likelihood fit

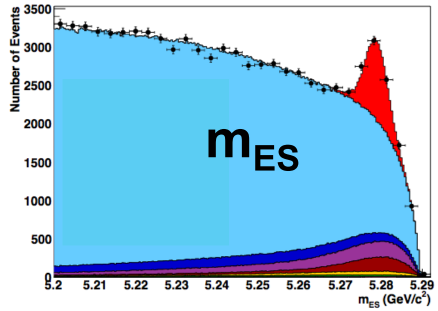

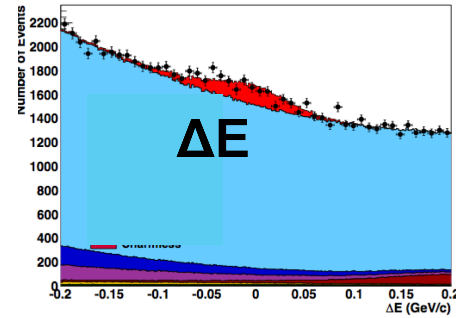

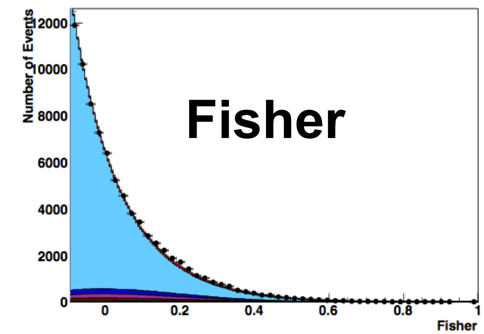

(2) Extraction of signal $m_{K\pi\pi}$ & $m_{K\pi}$ spectra

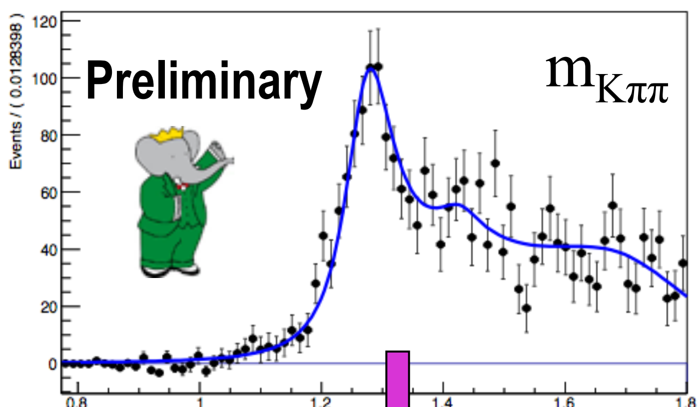

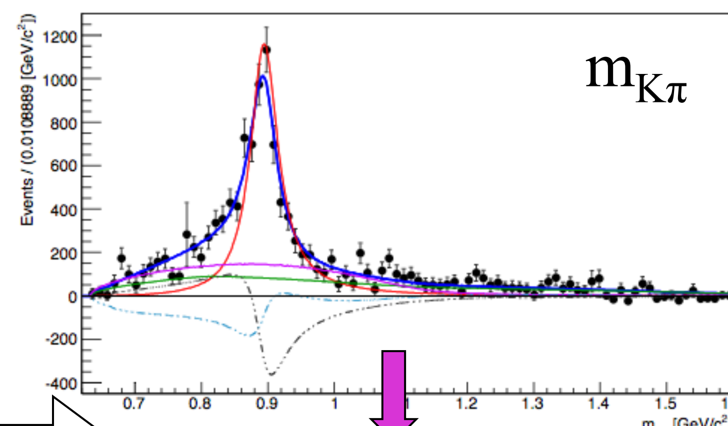

(3) Fit of $m_{K\pi\pi}$, $m_{K\pi}$ (projection) to **extract amplitudes**

$A(K_{res} \to K\pi\pi)$ ⇨ (input) ⇨ $A(K^*)$ $A(\rho)$…

Amplitudes ➔ dilution factor and branching fractions

The dilution factor

- From the fit to the $\mathbf{m_{K\pi}}$ spectrum of in the (charged) mode $\mathbf{B^+ \to K^+\pi^-\pi^+\gamma}$

$$\mathcal{D}_{K_S^0\rho\gamma} = \frac{\int \left[|A_\rho|^2 + \Re(A_\rho^* A_{K^{*+}}) + \Re(A_\rho^* A_{K^{*-}}) + \overbrace{\Re(A_{K^{*+}}^* A_{K^{*-}})}^{\propto \mathrm{FF}_{K^*}} + \overbrace{\Re(A_{(K\pi)^+}^* A_{(K\pi)^-})}^{\propto \mathrm{FF}_{(K\pi)_0}} \right]}{\int \left[\underbrace{|A_\rho|^2}_{\propto \mathrm{FF}_\rho} + \underbrace{\Re(A_\rho^* A_{K^{*+}}) + \Re(A_\rho^* A_{K^{*-}})}_{\propto \mathrm{FF}^{\mathrm{interf.}}_{K^*-\rho}} + \underbrace{\frac{|A_{K^{*+}}|^2 + |A_{K^{*-}}|^2}{2}}_{\propto \mathrm{FF}_{K^*}} + \underbrace{\frac{|A_{(K\pi)^+}|^2 + |A_{(K\pi)^-}|^2}{2}}_{\propto \mathrm{FF}_{(K\pi)_0}} \right]}$$

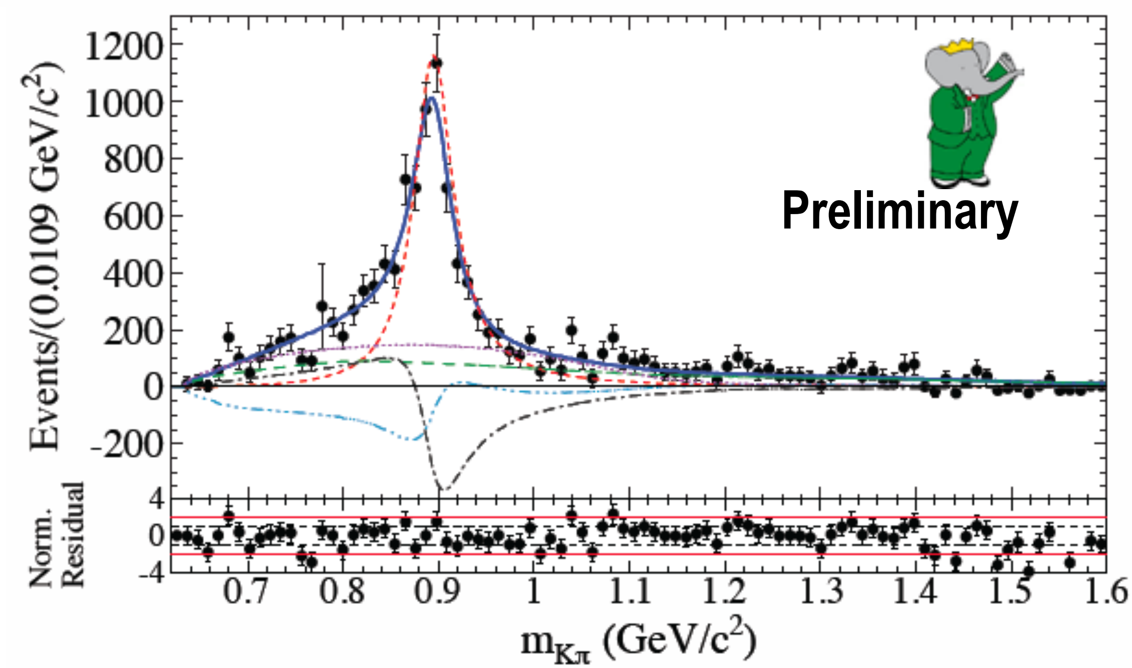

$$\boxed{\mathcal{D}_{K_S^0\rho\gamma} = 0.549^{+0.096}_{-0.094}}$$

- Total PDF
- $K^*(892)$
- $\rho^0(770)$
- $(K\pi)_0$ S-wave
- $K^*(892) - \rho^0(770)$ interf.
- $\rho^0(770) - (K\pi)_0$ interf.

$B \to K\pi^+\pi^-\gamma$

Results (BF in $B^+ \to K^+\pi^-\pi^+\gamma$)

Preliminary

$K_{res} \to K^+\pi^-\pi^+$

Mode	$\mathcal{B}(B^+ \to \text{Mode}) \times \mathcal{B}(K_{res} \to K^+\pi^+\pi^-) \times 10^{-6}$	$\mathcal{B}(B^+ \to \text{Mode}) \times 10^{-6}$	PDG values $(\times 10^{-6})$
Inclusive $B^+ \to K^+\pi^+\pi^-\gamma$	$\cdots$	$27.2 \pm 1.0^{+1.1}_{-1.3}$	27.6 ± 2.2
$K_1(1270)^+\gamma$	$14.5^{+2.0+1.1}_{-1.3-1.2}$	$44.0^{+6.0+3.5}_{-4.0-3.7} \pm 4.6$	43 ± 13
$K_1(1400)^+\gamma$	$4.1^{+1.9+1.3}_{-1.2-0.8}$	$9.7^{+4.6+3.1}_{-2.9-1.8} \pm 0.6$	< 15 CL$= 90\%$
$K^*(1410)^+\gamma$	$9.7^{+2.1+2.4}_{-1.9-0.7}$	$23.8^{+5.2+5.9}_{-4.6-1.4} \pm 2.4$	$\emptyset$
$K_2^*(1430)^+\gamma$	$1.5^{+1.2+0.9}_{-1.0-1.4}$	$10.4^{+8.7+6.3}_{-7.0-9.9} \pm 0.5$	14 ± 4
$K^*(1680)^+\gamma$	$17.0^{+1.7+3.5}_{-1.4-3.0}$	$71.7^{+7.2+15}_{-5.7-13} \pm 5.8$	< 1900 CL$= 90\%$

Resonances in $K^+\pi^-\pi^+$ system

Mode	$\mathcal{B}(B^+ \to \text{Mode}) \times \mathcal{B}(R \to hh) \times 10^{-6}$	$\mathcal{B}(B^+ \to \text{Mode}) \times 10^{-6}$	PDG values $(\times 10^{-6})$
Inclusive $B^+ \to K^+\pi^+\pi^-\gamma$	$\cdots$	$27.2 \pm 1.0^{+1.1}_{-1.3}$	27.6 ± 2.2
$K^{*0}(892)\pi^+\gamma$	$17.3 \pm 0.9^{+1.2}_{-1.1}$	$26.0^{+1.4}_{-1.3} \pm 1.8$	20^{+7}_{-6}
$K^+\rho(770)^0\gamma$	$9.1^{+0.8}_{-0.7} \pm 1.3$	$9.2^{+0.8}_{-0.7} \pm 1.3 \pm 0.02$	< 20 CL$= 90\%$
$(K\pi)_0^{*0}\pi^+\gamma$	$11.3 \pm 1.5^{+2.0}_{-2.6}$	$\cdots$	$\emptyset$
$(K\pi)_0^0\pi^+\gamma$ (NR)	$\cdots$	$10.8^{+1.4+1.9}_{-1.5-2.5}$	< 9.2 CL$= 90\%$
$K_0^*(1430)^0\pi^+\gamma$	$0.51 \pm 0.07^{+0.09}_{-0.12}$	$0.82 \pm 0.11^{+0.15}_{-0.19} \pm 0.08$	$\emptyset$

Results (BF in $B^+ \to K^+\pi^-\pi^+\gamma$)

$B \to K\pi^+\pi^-\gamma$

Preliminary

$K_{res} \to K^+\pi^-\pi^+$

Mode	$\mathcal{B}(B^+ \to \text{Mode}) \times \mathcal{B}(K_{res} \to K^+\pi^+\pi^-) \times 10^{-6}$	$\mathcal{B}(B^+ \to \text{Mode}) \times 10^{-6}$	PDG values ($\times 10^{-6}$)
Inclusive $B^+ \to K^+\pi^+\pi^-\gamma$	$\cdots$	$27.2 \pm 1.0^{+1.1}_{-1.3}$	27.6 ± 2.2
$K_1(1270)^+\gamma$	$14.5^{+2.0+1.1}_{-1.3-1.2}$	$44.0^{+6.0+3.5}_{-4.0-3.7} \pm 4.6$	43 ± 13
$K_1(1400)^+\gamma$	$4.1^{+1.9+1.3}_{-1.2-0.8}$	$9.7^{+4.6+3.1}_{-2.9-1.8} \pm 0.6$	< 15 CL$=90\%$
$K^*(1410)^+\gamma$	$9.7^{+2.1+2.4}_{-1.9-0.7}$	$23.8^{+5.2+5.9}_{-4.6-1.4} \pm 2.4$	$\emptyset$
$K_2^*($			14 ± 4
$K^*($			0 CL$=90\%$

Several of these measurements are the world best (or done for the first time)

Resonances in $K^+\pi^-\pi^+$ system

			DG values ($\times 10^{-6}$)
			27.6 ± 2.2
$K^{*0}(892)\pi^+\gamma$	$17.3 \pm 0.9^{+1.2}_{-1.1}$	$26.0^{+1.4}_{-1.3} \pm 1.8$	20^{+7}_{-6}
$K^+\rho(770)^0\gamma$	$9.1^{+0.8}_{-0.7} \pm 1.3$	$9.2^{+0.8}_{-0.7} \pm 1.3 \pm 0.02$	< 20 CL$=90\%$
$(K\pi)^{*0}_0\pi^+\gamma$	$11.3 \pm 1.5^{+2.0}_{-2.6}$	$\cdots$	$\emptyset$
$(K\pi)^0_0\pi^+\gamma$ (NR)	$\cdots$	$10.8^{+1.4+1.9}_{-1.5-2.5}$	< 9.2 CL$=90\%$
$K_0^*(1430)^0\pi^+\gamma$	$0.51 \pm 0.07^{+0.09}_{-0.12}$	$0.82 \pm 0.11^{+0.15}_{-0.19} \pm 0.08$	$\emptyset$

Results ($\mathcal{S}$)

B→Kπ⁺π⁻γ

- From the time-dependent analysis of the (neutral) decay mode **$B^0 \to K_S\pi^-\pi^+\gamma$**

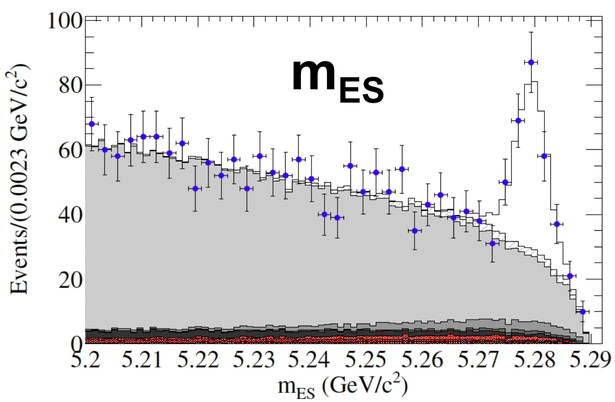

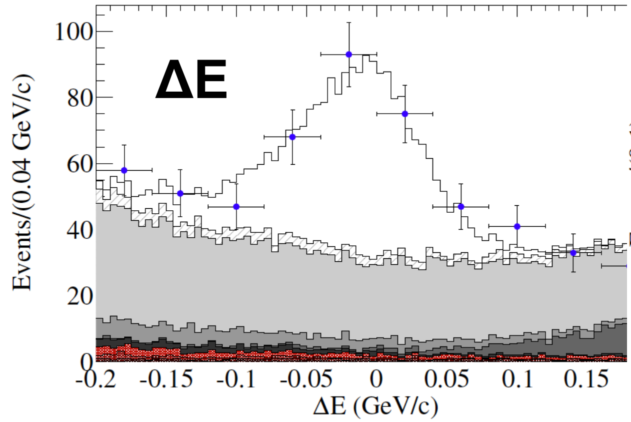

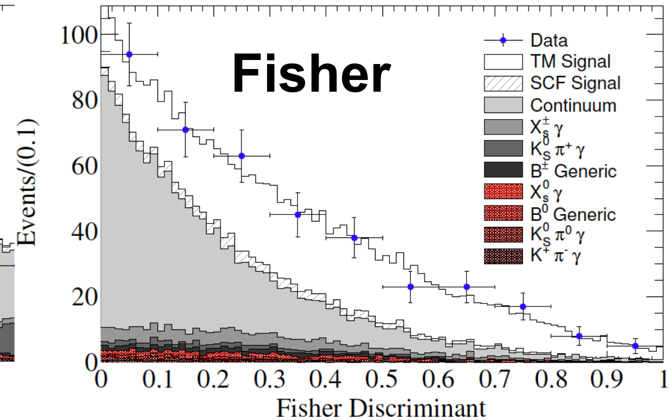

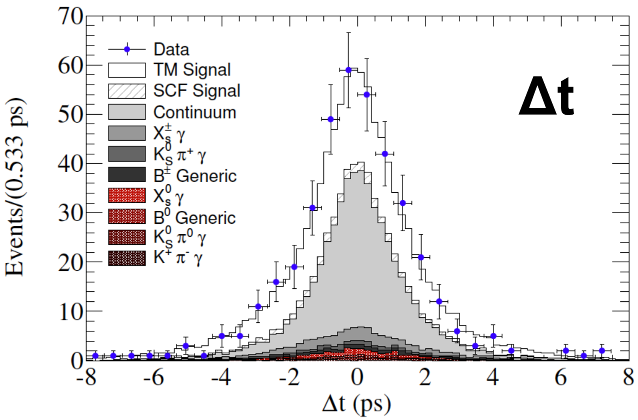

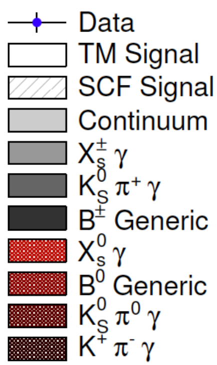

Preliminary

With present sensitivity, $\mathcal{S}$ in agreement with the SM prediction and with previous measurement from Belle

$$\mathcal{S}_{K_S^0\rho\gamma} = \frac{\mathcal{S}_{K_S^0\pi^+\pi^-\gamma}}{\mathcal{D}_{K_S^0\rho\gamma}} = 0.249 \pm 0.455^{+0.076}_{-0.060}$$

$$\mathcal{S}_{K_S^0\rho^0\gamma} \overset{\text{SM}}{\sim} 0.02$$

Summary and Conclusions

- Babar continues to produce exciting physics results, adding more information and using more sophisticated analysis techniques to improve the precision of measurements in radiative-penguin B decays
- All measurements presented here agree with the standard model predictions
- Larger samples are needed to tell whether or not there could be indications for NP. The analyses shown here have interesting perspectives with more data (Belle II and LHCb)

Extras

BF results and SM predictions

- Calculation of the fully inclusive $B \to X_s \ell^+ \ell^-$ rate is complicated by the presence of the charmonia, and the latest SM calculation is a decade old

(4.6 +/- 0.8) x 10^{-6} Nucl.Phys.B 685, 351 (2004)

- Theory efforts have instead been directed to the (theoretically clean) perturbative window $1 < q^2 < 6$ GeV^2/c^4

Theory

$$\mathcal{B}(B \to X_s \mu^+ \mu^-) = (1.59 \pm 0.11) \times 10^{-6}$$
$$\mathcal{B}(B \to X_s e^+ e^-) = (1.64 \pm 0.11) \times 10^{-6}$$

T. Huber, T. Hurth and E. Lunghi, Nucl. Phys. B **802**, 40 (2008).

Our results

$$\left.\begin{array}{ll} X_s\,\mu^+\mu^- & 0.66^{+0.82}_{-0.76}{}^{+0.30}_{-0.24} \pm 0.07 \\ X_s\,e^+e^- & 1.93^{+0.47}_{-0.45}{}^{+0.21}_{-0.16} \pm 0.18 \\ X_s\,\ell^+\ell^- & 1.60^{+0.41}_{-0.39}{}^{+0.17}_{-0.13} \pm 0.18 \end{array}\right\} \times 10^{-6}$$

- and the region above the $\psi(2S)$ ($q^2 > 14.2$ GeV^2/c^4) :

Theory

$$\mathcal{B}(\bar{B} \to X_s \mu\mu)_{\text{high}} = (2.40^{+0.69}_{-0.62}) \times 10^{-7}$$

T. Huber, T. Hurth and E. Lunghi, Nucl. Phys. B **802**, 40 (2008).

Our results

$$\left.\begin{array}{ll} X_s\,\mu^+\mu^- & 0.60^{+0.31}_{-0.29}{}^{+0.05}_{-0.04} \pm 0.00 \\ X_s\,e^+e^- & 0.56^{+0.19}_{-0.18}{}^{+0.03}_{-0.03} \pm 0.00 \\ X_s\,\ell^+\ell^- & 0.57^{+0.16}_{-0.15}{}^{+0.03}_{-0.02} \pm 0.00 \end{array}\right\} \times 10^{-6}$$

BF results and SM predictions

- Our measured BF in the high mass region $q^2 > 14.2$: >2σ away from the prediction related to the δC_9 NP interpretation of the recently reported LHCb P_5' anomaly in $B^0 \to K^* \mu^+ \mu^-$

Our result

Bin	Range	$B \to X_s \ell^+ \ell^-$
q_0^2	$1.0 < q^2 < 6.0$	$1.60^{+0.41}_{-0.39}{}^{+0.17}_{-0.13} \pm 0.18$
q_1^2	$0.1 < q^2 < 2.0$	$2.70^{+0.45}_{-0.42}{}^{+0.21}_{-0.16} \pm 0.35$
q_2^2	$2.0 < q^2 < 4.3$	$0.46^{+0.26}_{-0.23}{}^{+0.10}_{-0.06} \pm 0.07$
q_3^2	$4.3 < q^2 < 6.8$	$0.60^{+0.27}_{-0.25}{}^{+0.10}_{-0.08} \pm 0.05$
q_4^2	$10.1 < q^2 < 12.9$	$1.02^{+0.32}_{-0.30}{}^{+0.10}_{-0.07} \pm 0.04$
q_5^2	$14.2 < q^2$	$0.57^{+0.16}_{-0.15}{}^{+0.03}_{-0.02} \pm 0.00$
$m_{X_s,1}$	$0.4 < m_{X_s} < 0.6$	$0.71^{+0.15}_{-0.14}{}^{+0.03}_{-0.03} \pm 0.00$
$m_{X_s,2}$	$0.6 < m_{X_s} < 1.0$	$1.02^{+0.27}_{-0.25}{}^{+0.06}_{-0.05} \pm 0.00$
$m_{X_s,3}$	$1.0 < m_{X_s} < 1.4$	$1.32^{+0.61}_{-0.58}{}^{+0.19}_{-0.15} \pm 0.05$
$m_{X_s,4}$	$1.4 < m_{X_s} < 1.8$	$1.36^{+0.67}_{-0.63}{}^{+0.50}_{-0.34} \pm 0.12$
Total	$0.1 < q^2$	$6.73^{+0.70}_{-0.64}{}^{+0.34}_{-0.25} \pm 0.50$

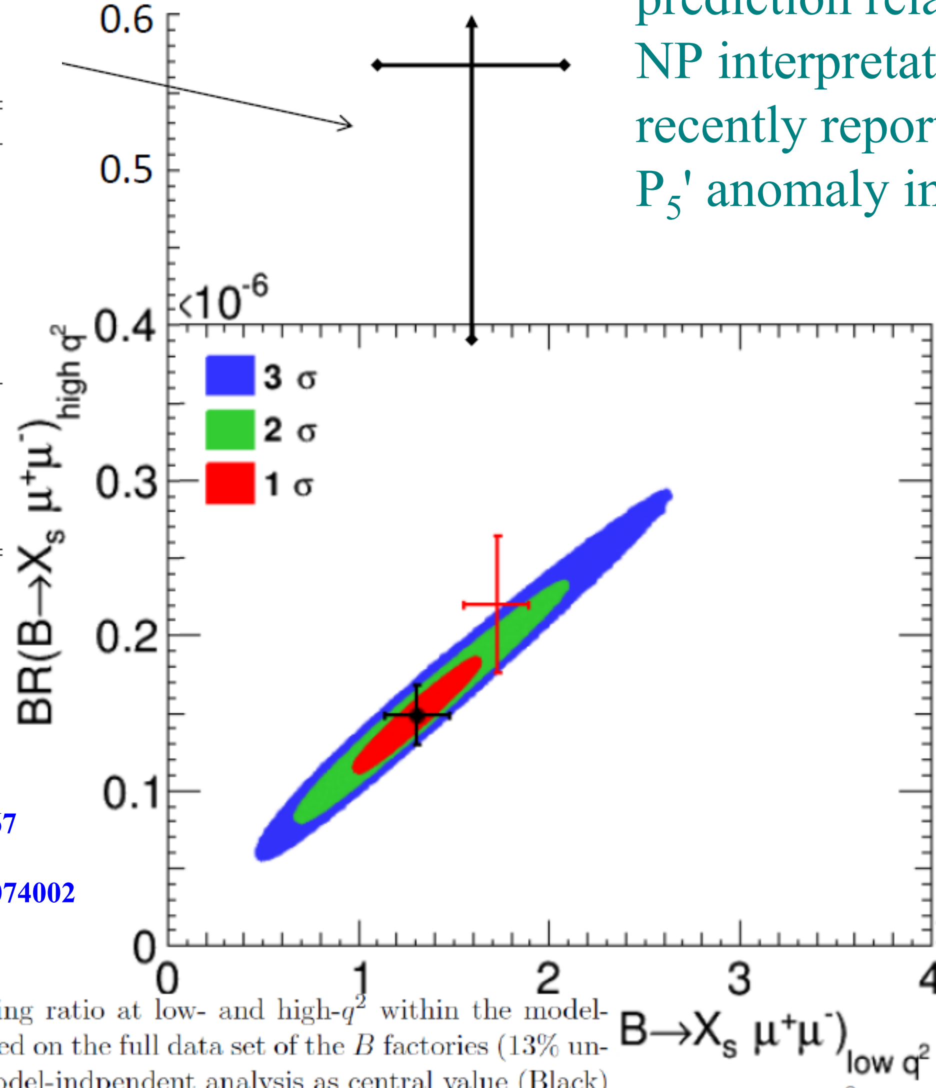

T. Hurth and F. Mahmoudi, arXiv:1312.5267
based on model independent fit from
S. Descotes-Genon et al., Phys. Rev. D88 (2013) 074002

Figure 3: 1-,2-,and 3-σ ranges for the branching ratio at low- and high-q^2 within the model-independent analysis. Future measurement based on the full data set of the B factories (13% uncertainty) assuming the best-fit point of the model-indpendent analysis as central value (Black) and the SM predictions (Red).

Effective Hamiltonian

$$H_{eff} = -\frac{4G_F}{\sqrt{2}} V_{tb} V_{ts}^{*} \sum_i \Big[\underbrace{C_i(\mu) O_i(\mu)}_{\text{left -handed part}} + \underbrace{C_i'(\mu) O_i'(\mu)}_{\substack{\text{right -handed part} \\ \text{suppressed in SM}}} \Big]$$

$i = 1,2$	Tree
$i = 3-6,8$	Gluon penguin
$i = 7$	Photon penguin
$i = 9,10$	Electroweak penguin
$i = S$	Higgs (scalar) penguin
$i = P$	Pseudoscalar penguin

Tests with J/ψ and ψ(2S) samples

$B \to X_s \ell^+ \ell^-$

- A_{CP} of vetoed J/ψ dataset: 0.0046±0.0057
- Comparison of likelihood ratio distributions in data and MC:

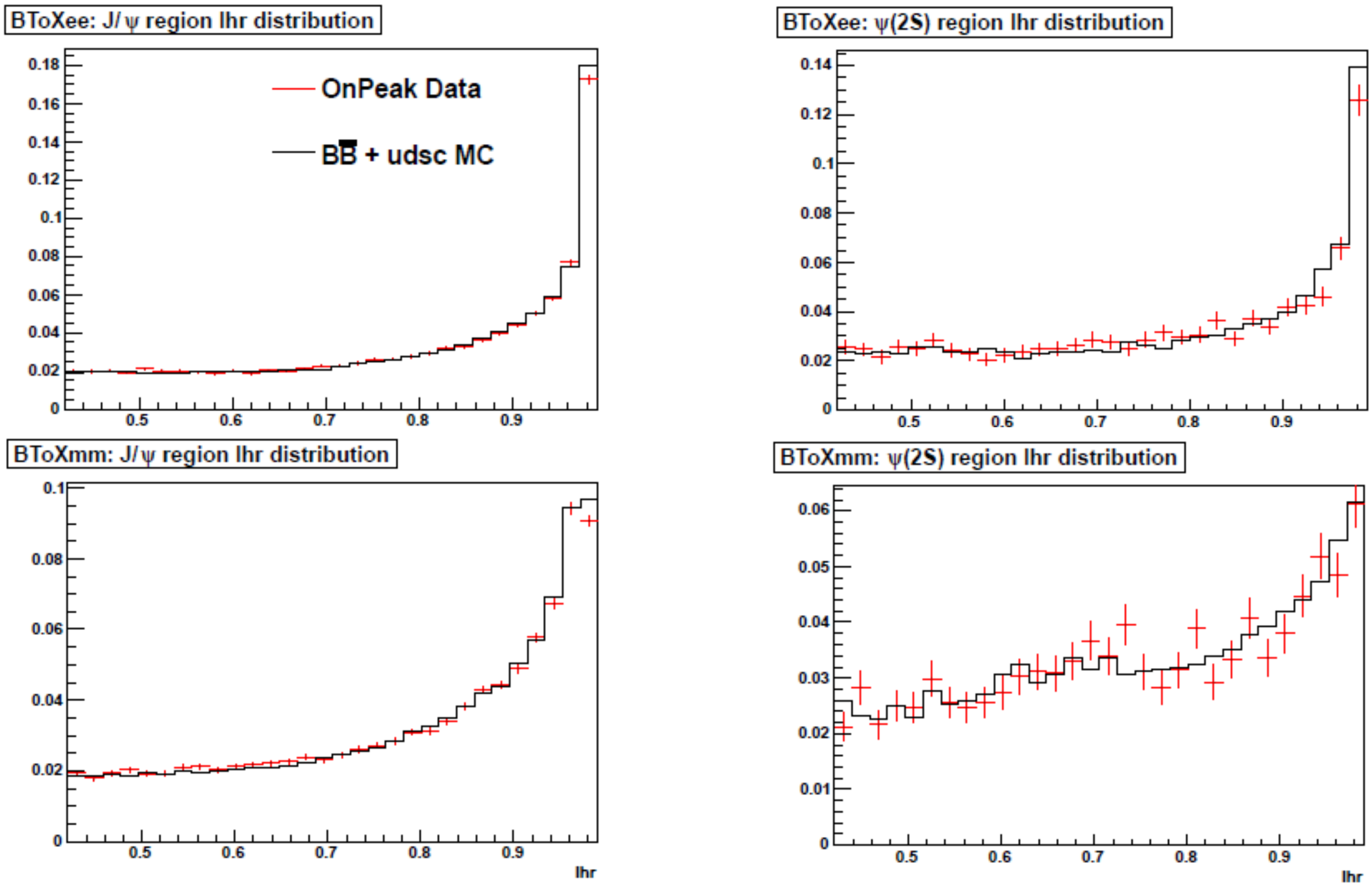

Extrapolation to fully inclusive rate

- A scaling factor derived from the ratio of unseen to seen events in simulated $B \to X_s l^+ l^-$ signal events is used to scale the measured BF into the total BF

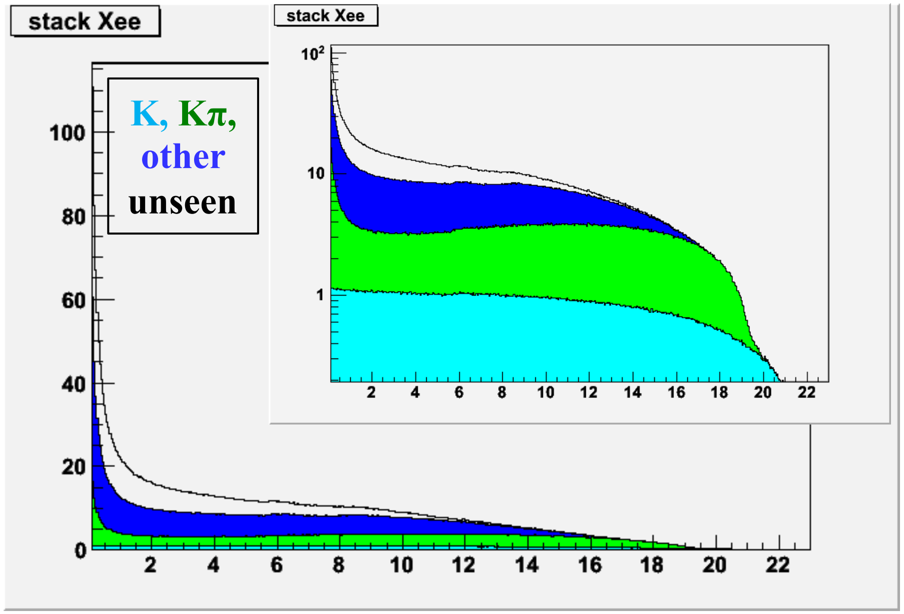

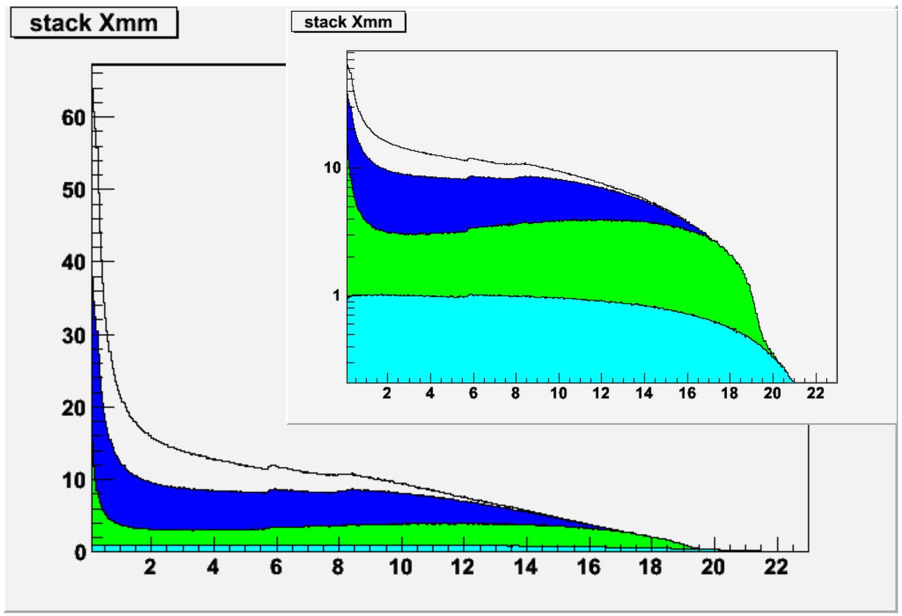

Systematics

- Systematics are grouped into three categories:
  - Possible biases arising from uncertainties in the fit model pdf parameterizations and normalizations, affecting the fitted raw signal yields;
  - Systematics affecting the calculation of un-extrapolated branching fractions, e.g. BB counting, reconstruction efficiencies, etc.;
  - Systematics associated with the unseen scaling factor derived from the underlying event generator model are characterized using
    - 20 *a priori* generator-level variations in b-quark mass and Fermi motion parameter, and hadronization of the X_s system by JETSET; and
    - *a posteriori* variations of ±50% in the π^0, π^+ and kaon multiplicities from the nominal generator model.

$M_{K\pi\pi}$ fit model

- **Model:**
  - Five resonances modeled by BW (mean and width fixed to PDG values):

J^P	K_{res}	Mass m_j^0 (MeV/c^2)	Width Γ_j^0 (MeV/c^2)
1^+	$K_1(1270)$	1272 ± 7	90 ± 20
	$K_1(1400)$	1403 ± 7	174 ± 13
1^-	$K^*(1410)$	1414 ± 15	232 ± 21
	$K^*(1680)$	1717 ± 27	322 ± 110
2^+	$K_2^*(1430)$	1425.6 ± 1.5	98.5 ± 2.7

$$\text{BW}_j^J(m) = \left.\frac{1}{(m_j^0)^2 - m^2 - i m_j^0 \Gamma_j^0}\right|_{m=m_{K\pi\pi}}$$

$$|A(m;c_j)|^2 = \left.\sum_{\boxed{J}} \left| \sum_j c_j \, \text{BW}_j^J(m) \right|^2 \right|_{m=m_{K\pi\pi}}$$

$$c_j = \alpha_j \, e^{i\phi_j}$$

- **Fit to $K\pi\pi$ invariant mass sPlot (binned) distribution**
  - 8 fitted parameters:
    - ➜ 4 magnitudes, 2 relative phases
    - ➜ 2 widths ($K_1(1270)$ and $K^*(1680)$)
  - Due to the integration over the angular variables, only resonances with same J^P interfere
  - Randomized initial parameter values
- **Fit fractions computed from magnitudes and phases**

Efficiency Correction of $M_{K\pi}$

- Need to correct the 2-dimensional $m_{K\pi}$-$m_{\pi\pi}$ signal sPlot **(A)**
- Built $m_{K\pi}$-$m_{\pi\pi}$ efficiency maps for each $K_{res} \to K\pi\pi$
- Checked that efficiency maps were not correlated to m_{Kpipi}
- Combine them using weights extracted from data **(B)**
- Used projection on $m_{K\pi}$ for the fit **(C)**

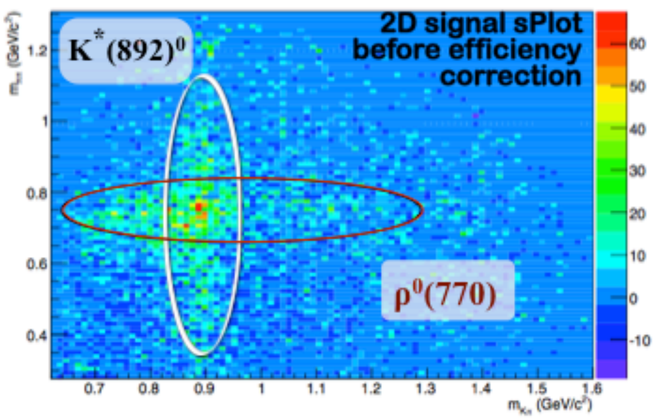

(A)

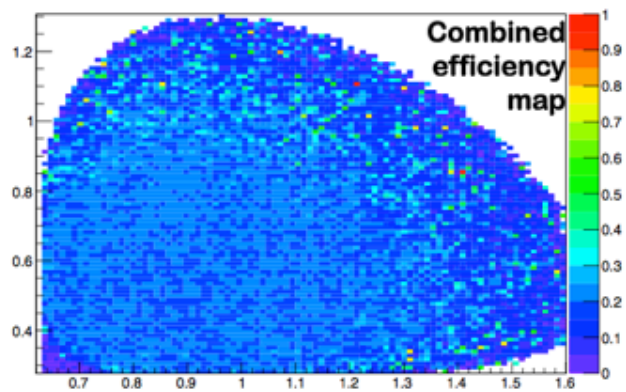

(B)

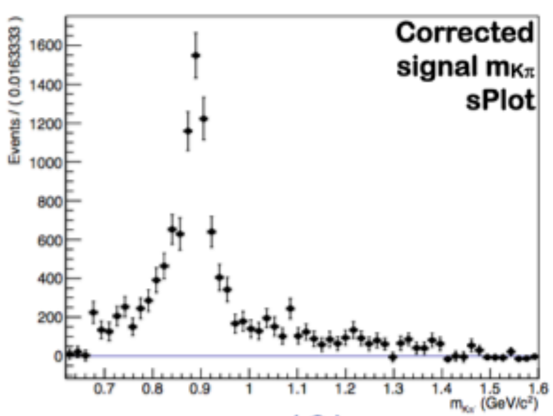

(C)

Lineshapes in $M_{K\pi}$ fit

- Based on generator level MC, with input from $M_{K\pi\pi}$ fit
- Takes into account large distortions due to phase space

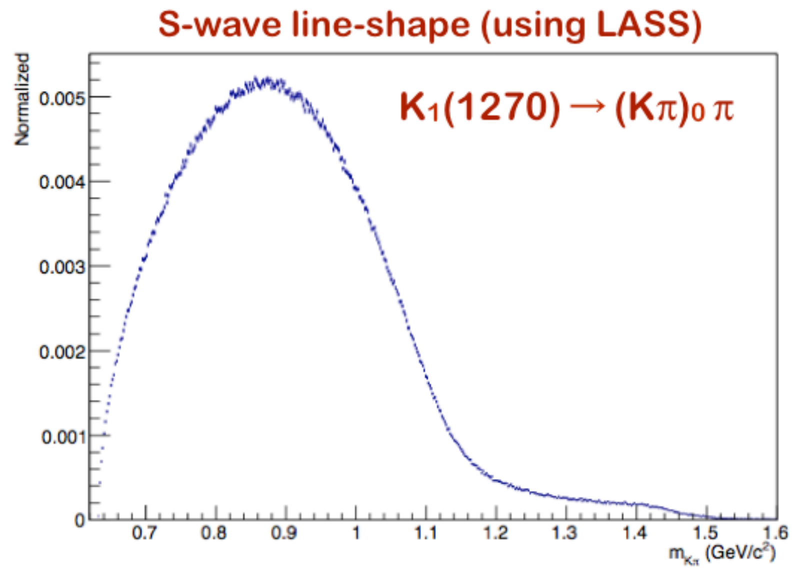

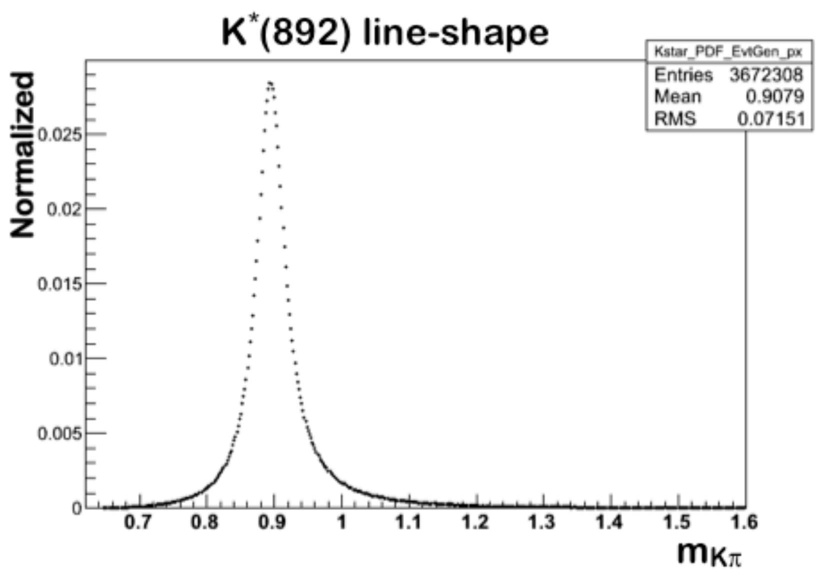

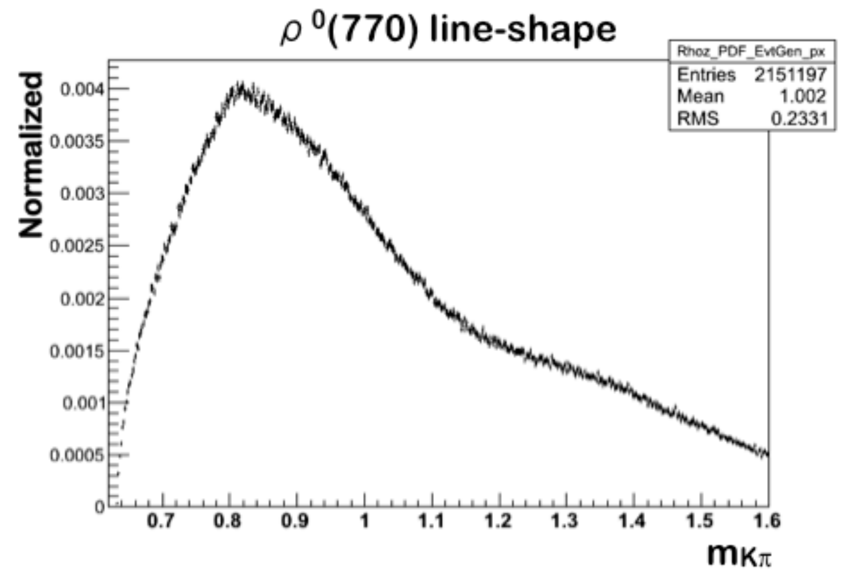

$M_{K\pi}$ fit model (I)

Total PDF:

- Coherent sum of $K^*(892)$, $\rho^0(770)$ and $K\pi$ S-wave component:

$$|A(m_{K\pi};c_j)|^2 = \left| \int_{m_{\pi\pi}^{min}}^{m_{\pi\pi}^{max}} \left(\sum_j c_j \sqrt{\mathrm{H}_{\mathrm{R}_j}(m_{K\pi}, m_{\pi\pi})}\, e^{i\Phi_{\mathrm{R}_j}(m)} \right) dm_{\pi\pi} \right|^2 , \quad c_j = \alpha_j\, e^{i\phi_j}$$

$$= |c_{K^*}|^2 \mathcal{H}_{K^*} + |c_{\rho^0}|^2 \mathcal{H}_{\rho^0} + |c_{(K\pi)_0}|^2 \mathcal{H}_{(K\pi)_0} + I$$

- Invariant-mass-dependent magnitude defined as the projection of two-dimensional histograms:

$$\mathcal{H}_{R_j}(m_{K\pi}) = \int_{m_{\pi\pi}^{min}}^{m_{\pi\pi}^{max}} H_{R_j}(m_{K\pi}, m_{\pi\pi})\, dm_{\pi\pi}.$$

- The invariant-mass-dependent phase is taken from the analytical expression of the corresponding line shape:

$$\Phi_{\mathrm{R}_j}(m) = \arccos\left(\frac{\Re[\mathrm{R}_j(m)]}{|\mathrm{R}_j(m)|} \right) \Leftrightarrow \begin{cases} m = m_{K\pi} \;\Rightarrow\; \text{$\mathrm{R}_j(m_{K\pi})$ is taken as RBW for $K^{*0}(892)$ and as LASS for S-wave ,} \\ m = m_{\pi\pi} \;\Rightarrow\; \text{$\mathrm{R}_j(m_{\pi\pi})$ is taken as a GS line shape for $\rho^0(770)$,} \end{cases}$$

$M_{K\pi}$ fit model (II)

$B \to K\pi^+\pi^-\gamma$

Interference:

- **Interference terms:**

$$
\begin{aligned}
I(m_{K\pi}; c_{\rho^0}, c_{(K\pi)_0}) \;=\; & 2\alpha_{\rho^0}\Big[\cos(\phi_{\rho^0} - \Phi_{\mathrm{RBW}}) \int_{m_{\pi\pi}^{min}}^{m_{\pi\pi}^{max}} \sqrt{\mathrm{H}_{\rho^0}\mathrm{H}_{K^*}} \cos(\Phi_{\mathrm{GS}})\, dm_{\pi\pi} \\
& - \sin(\phi_{\rho^0} - \Phi_{\mathrm{RBW}}) \int_{m_{\pi\pi}^{min}}^{m_{\pi\pi}^{max}} \sqrt{\mathrm{H}_{\rho^0}\mathrm{H}_{K^*}} \sin(\Phi_{\mathrm{GS}})\, dm_{\pi\pi}\Big] \\
& + 2\alpha_{\rho^0}\alpha_{(K\pi)_0}\Big[\cos(\phi_{\rho^0} - \phi_{(K\pi)_0} - \Phi_{\mathrm{LASS}}) \int_{m_{\pi\pi}^{min}}^{m_{\pi\pi}^{max}} \sqrt{\mathrm{H}_{\rho^0}\mathrm{H}_{(K\pi)_0}} \cos(\Phi_{\mathrm{GS}})\, dm_{\pi\pi} \\
& - \sin(\phi_{\rho^0} - \phi_{(K\pi)_0} - \Phi_{\mathrm{LASS}}) \int_{m_{\pi\pi}^{min}}^{m_{\pi\pi}^{max}} \sqrt{\mathrm{H}_{\rho^0}\mathrm{H}_{(K\pi)_0}} \sin(\Phi_{\mathrm{GS}})\, dm_{\pi\pi}\Big]
\end{aligned}
$$

Term describing interference between the $K^*(892)$ and $\rho^0(770)$ amplitudes

Term describing interference between the $\rho^0(770)$ and $(K\pi)$ S-wave amplitudes

Interference vanishes between the S-wave and the $K^*(892)$

Time dependent CP parameters (I)

$B \to K\pi^+\pi^-\gamma$

- Measured the time-dependent CP asymmetry parameters in the decay $B^0 \to K_S\pi^-\pi^+\gamma$ with the full BaBar dataset

(with $m_{K\pi\pi} < 1.8$ GeV/c², $0.6 < m_{\pi\pi} < 0.9$ GeV/c², $m_{K\pi} < 0.845$ GeV/c² and $m_{K\pi} > 0.945$ GeV/c²)

$$\boxed{\begin{aligned} \mathcal{S}_{K^0_S\pi^+\pi^-\gamma} &= 0.137 \pm 0.249(\text{stat.})^{+0.042}_{-0.033}(\text{syst.}) \\ \mathcal{C}_{K^0_S\pi^+\pi^-\gamma} &= -0.390 \pm 0.204(\text{stat.})^{+0.045}_{-0.050}(\text{syst.}) \end{aligned}}$$

$$\begin{aligned} \mathcal{S}^{\text{Belle}}_{K^0_S\pi^+\pi^-\gamma} &= 0.09 \pm 0.27(\text{stat.})^{+0.04}_{-0.07}(\text{syst.}) \\ \mathcal{C}^{\text{Belle}}_{K^0_S\pi^+\pi^-\gamma} &= -0.05 \pm 0.18(\text{stat.}) \pm 0.06(\text{syst.}) \end{aligned}$$

Comparable error on the effective CP asymmetry parameters compared to Belle's results
(with ~1.4 times less events in the present analysis)

$B \to K\pi^+\pi^-\gamma$

Time dependent CP parameters (II)

- The mixing induced CP violation parameter for $B^0 \to K_S \rho^0 \gamma$ decays:

$$\boxed{\mathcal{S}_{K^0_S\rho\gamma} = \frac{\mathcal{S}_{K^0_S\pi^+\pi^-\gamma}}{\mathcal{D}_{K^0_S\rho\gamma}} = 0.249 \pm 0.455^{+0.076}_{-0.060}}$$

Paper in prep.

- Compared with other CPV measurements in radiative decays:

$$\mathcal{S}^{\mathrm{Belle}}_{K^0_S\rho\gamma} = 0.11 \pm 0.33^{+0.05}_{-0.09}$$

PhysRevLett.101.251601

$$\mathcal{S}^{\mathrm{BABAR}}_{K^0_S\pi^0\gamma} = -0.78 \pm 0.59 \pm 0.09$$

PhysRevD.78.071102

$$\mathcal{S}^{\mathrm{Belle}}_{K^0_S\pi^0\gamma} = -0.10 \pm 0.31 \pm 0.07$$

PhysRevD.74.111104